Earthquakes and Structures, *Vol. 16, No. 4 (2019) 375-389*
DOI: https://doi.org/10.12989/eas.2019.16.4.375

Comparative study on retrofitting strategies for residential buildings after earthquakes

Mengqi Yang[1a] and Chi Zhang[*1,2]

[1]*School of Geographical Sciences, Gangzhou University, Guangzhou, Guangdong, 510006, China*
[2]*School of Geography, South China Normal University, Guangzhou, Guangdong, 510631, China*

(Received January 17, 2019, Revised February 17, 2019, Accepted February 20, 2019)

Abstract. During earthquakes, the performance of structures needs to be evaluated, which provides guidance for selecting suitable retrofitting schemes. The purpose of this paper is to accomplish seismic assessment of a simple steel residential building. Once the responses of the system are determined, the scope of the study extends to evaluate selected retrofitting strategies that are intended to rehabilitate the flaws of the structure under prescribed ground motions with high probability of occurrence at the site. After implementing the retrofits, seismic assessment of the upgraded structure is carried out to check if the remediation at various seismic performance levels is acquired or not. Outcomes obtained from retrofitted scenarios are compared to the results obtained from the initial un-retrofitted configuration of the structure. This paper presents the process for optimal selection of rehabilitation solutions considering the cost of implementation, downtime and disruption to property owners while improving the seismic performance level of the structure.

Keywords: seismic assessment; retrofitting; passive damper; base isolation; structural weakening

1. Introduction

Structural design according to old practice was principally based on gravity load distribution without proper consideration for earthquake forces. Seismic assessment of existing structures is needed, since they possess much more potential threats compared to seismically designed new constructions following recent codes. Therefore, the performance of structures should be evaluated especially for those in vulnerable areas prone to seismic hazards. As a result, strengthening operations should be implemented to those structures that have high possibility to failure during earthquakes.

The concept of seismic design and assessment based on limit displacements has been gaining credence over the past 20 years, as it has become appreciated that structural damage can be directly related to strains (and hence by integration to displacements), and non-structural damage, in buildings at least, can be related to drifts (Priestley *et al.* 2005). Displacement-based design (Calvi and Kingsley 1995, Kowalsky *et al.* 1995, Priestley and Kowalsky 2000, Panagiotakos and Fardis 2001, Fardis 2007, Priestley *et al.* 2007, Calvi and Sullivan 2009) emerges as opposed to force-based approaches, both of which could be used to evaluate the performance of structures. Force-based method requires an assumption of force-reduction factor involving no real strength, ductility and energy dissipation. In addition, structures do not respond elastically most of the time during earthquakes. Conversely, direct displacement-based procedure is sufficient to catch the real seismic behaviour of structures and encouraging results have been obtained for single degree of freedom systems, frame and structural wall buildings (Priestley 1997, Priestley *et al.* 2007), and bridges (Cardone *et al.* 2011, Tubaldi and Dall'Asta 2011, Şadan *et al.* 2012, Della Corte *et al.* 2013). These analyses neglect the complex soil-structure interaction effects. Some recent investigations show that nonlinearity occurring at sub-structure level could be detrimental to structures (Ciampoli and Pinto 1995, Mylonakis and Gazetas 2000, Ni 2012). The extension of direct displacement-based approaches to consider the soil-structure interaction effects has been conducted for reinforced concrete multi-span bridges with single-column piers (Ni 2013, Paolucci *et al.* 2013, Ni *et al.* 2014). The complexity of these approaches prevents the application of use in practice. Alternatively, nonlinear static analysis allows estimating the seismic demand within acceptable computational efforts, which can be compared with the capacity of all structural components according to the design codes (Ni 2014). However, the calculation of capacity is often problematic since the structure is different from the design drawing due to variables, such as corrosion or changes that are implemented during the construction. In principle, performing nonlinear time-history analysis or incremental dynamic analysis (Vamvatsikos and Cornell 2002) is the most correct approach, which provides the seismic demand and capacity at the same time.

Conventionally, structures subjected to earthquakes are analyzed using deterministic approaches. Recently, researchers focus more on the use of probabilistic methods, where the probability of failure due to earthquake excitation can be estimated (Ni *et al.* 2012, Sahu *et al.* 2019). The

*Corresponding author, Research Fellow
E-mail: xuejinghutian123@sina.com
[a]Research Fellow

http://www.techno-press.com/journals/eas&subpage=7
ISSN: 2092-7614 (Print), 2092-7622 (Online)

Monte Carlo technique is a typical approach to conduct probabilistic analysis for structures under earthquakes, in which the input parameters are varied following predefined probability distribution functions. In general, a very large number of analyses (e.g., 1 million) need to be carried out to cover the probability space (Ni *et al.* 2018). The computational efforts of Monte Carlo simulation often hinder the probabilistic analysis. Recently, researchers adopted machine learning-based methods to simplify the calculation procedure, which can provide the probability of failure in a much shorter time (Mangalathu and Burton 2018, Mangalathu and Jeon 2018, Ni and Mangalathu 2018, Ni *et al.* 2018).

Flaws in the structural system determined during the assessment process could indicate the corresponding types of retrofitting strategies required. Various strategies were proposed to enhance the seismic performance of structures (Di Sarno and Elnashai 2003, 2005). Global interventions, such as structural walls and steel bracings, have been proved as efficient approaches to deal with the seismic upgrade of structures (Di Sarno and Elnashai 2009). However, these conventional strengthening schemes introduce additional lateral stiffness, which attract lateral forces to the structure. Injection of epoxy resin, shotcreting and incorporating FRP composites are the representative methods of member intervention strategies (Ghobarah and Abou-Elfath 2001, Pinho 2001, Elenas and Vasiliadis 2002, Faella *et al.* 2004, Griffith 2008). Specifically, the advantages of energy dissipation devices have been recognized (Constantinou *et al.* 1998, Kim *et al.* 2003, Christopoulos and Filiatrault 2006, Cimellaro *et al.* 2009, Di Sarno and Manfredi 2012). Base isolation also exhibits beneficial effects to help resisting seismic excitations without changing the structural configurations (Constantinou 2004).

The objective of this paper is to present the process for optimal selection of rehabilitation solutions for a simple steel residential building. The performance of this structure is evaluated numerically using nonlinear time-history analyses. Comparative study is conducted for energy dissipation devices (i.e., hysteretic, viscous and tuned mass dampers), base isolation and structural weakening techniques to help selecting the optimal solution. The efficiency of proposed procedures in reducing three parameters in terms of peak interstorey drifts, residual interstorey drifts and peak absolute floor accelerations is discussed. In addition, other criteria with regard to implementation efforts, additional intervention to foundation, cost of retrofitting, the matter of occupants and their relocation, downtime and aesthetics should be taken into account. The relevance of criteria strictly depends on the specific application and, moreover, they often represent trade-offs. All solutions will be implemented to the system and finally seismic assessment of the retrofitted structure will be carried out again to check if the rehabilitation is acquired or not.

2. Building description and modeling

This section describes a typical low-rise steel residential building before seismic evaluation of the structure is initiated. It has five storeys and is formed of five frames and three bays. The building has a regular form in plan and elevation. In the East-West direction, there are two exterior moment-resisting frames, one in each side, to resist lateral earthquake forces, whereas the internal frames only withstand the gravity loads. It is probably better to brace the weak direction (i.e., the North-South direction) in reality, but the purpose of this study is to evaluate different retrofitting schemes, which need to be implemented to a structure that has flaws. Fig. 1 displays the plan view of the building with dimensions and the elevation view of the moment resisting frame with storey heights and span lengths.

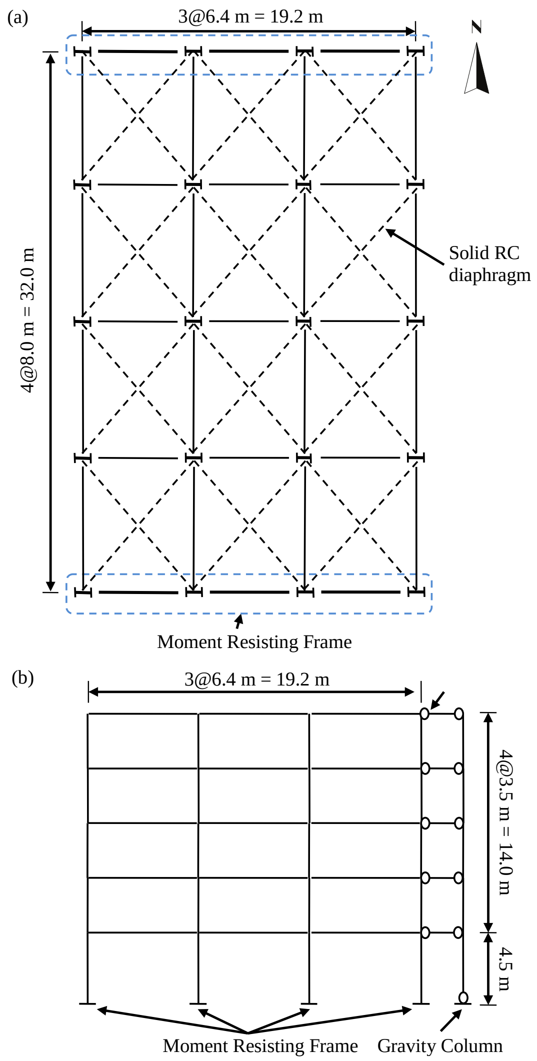

Fig. 1 Schematics: (a) plan view of the simple building and (b) elevated view of moment resisting frame

This paper aims at providing a methodology for optimal selection of rehabilitation solutions for a simple residential building. The primary idea is to select ground motions that have a probability of not exceeding desired adverse responses for any similar seismic intensity levels. Thus, the expected peak ground acceleration for the site is assigned to be 0.4 g to induce 90th percentile response at a design basis earthquake with a returning period of 475 years (Dhakal *et*

Table 1 Beam and column sections

Storey level	5th and 4th	3rd	2nd and 1st
Beam	W10×10×77	W12×12×79	W14×14.5×90
Exterior column	W18×11×86	W24×9×94	W27×10×114
Interior column	W24×12.75×131	W30×10.5×148	W36×12×170

al. 2006). The structure is designed to withstand uniformly distributed dead loads at roof level of 4.42 kPa and at floor levels of 4.67 kPa. Based on Eurocode 1 (CEN 2002), uniformly distributed live loads of Category B type buildings vary from 2 to 3 kPa. The maximum value of 3 kPa is selected to be imposed to the floor levels and 1 kPa is assigned for roof level. Modified live load reduction factors of 0.6 and 0.4 are applied afterwards as prescribed for floor and roof levels, respectively. The design uses EN 10025-2 S355 steel, which has the modulus of elasticity of 200 GPa, shear modulus of 78 GPa, specified minimum yield stress of 355 MPa and specified minimum tensile strength of 510 MPa. Table 1 illustrates the beam and column sections at each storey level.

A representative model of the structure for seismic evaluation of the present state is required. For this purpose, the dynamic analysis software package, Ruaumoko2D (Carr 2005) is selected to simulate the structure as precise as possible. Panel zones are modeled using bilinear rotational springs at the nodes between structural members (Kim and Engelhardt 2002), such that moment and shear can be transferred through beams and columns. It should be noted that a weak panel zone in shear can be detrimental to the structure that stress concentration at joints could potentially lead to fractures due to excessive rotations. A strong panel zone is therefore assumed to enable inelastic deformations occurring in plastic hinge regions in frame members (Krawinkler and Mohasseb 1987). This study is not to fully investigate the mechanism at panel zones, unless complex 3D finite element simulation is conducted (El-Tawil *et al.* 1999). Therefore, the effect of accidental torsion (even for symmetric buildings) on seismic analysis and design of the structure is neglected. The presence of reinforced concrete slab results in rigid diaphragmatic action. Subsequently, only half of the building is modeled due to symmetry of the structure. One exterior moment resisting frame is simulated, at Fig. 1. A gravity column has all the weights from interior frames, and is horizontally constrained to the moment resisting frame with hinges on both sides of the members. The base of the gravity column is pinned to the ground surface, so that there is no moment transfer to the gravity column. The ground level columns of exterior frame are assumed to have rigid connection to the soil and hence the soil-structure interaction is neglected. Inelastic response is enabled in plastic hinges that are permitted to form at both ends of frame members. Stiffness and strength deterioration due to local buckling in plastic hinges is considered indirectly by defining the plastic hinge length and properties. Bi-linear hysteretic behaviour is assigned for plastic hinges, where a curvature strain-hardening ratio of 2% is considered to modify the moment-rotation/curvature relationships. Their length is set equal to 90% of the associated member depth (Martínez-Rodrigo and Filiatrault 2015). Gusset plate rotational behaviour is not modelled as well as many other important factors influencing the behaviour of steel structures, since this parametric study is to compare the efficiency of different retrofitting strategies rather than going to a higher complex model. It should be emphasized that a two-dimensional model is established for the low-rise building subjected to different levels of earthquakes, because of the difficulty associated with the implementation of different retrofitting techniques in the numerical model. Although the building is simple, different retrofitting techniques are difficult to model. The complexity of the numerical model could add uncertainties in assumptions by introducing some additional input variables and it will require more computational efforts (storage and time).

3. Structural seismic performance

3.1 Seismic input

Pseudo-displacement response spectra can be derived from acceleration spectra by a crude multiplication factor $(T/2\pi)^2$. In reality, acceleration spectrum is not as sensitive as its displacement counterpart to filtering (Elnashai and Di Sarno 2008). This approximation often leads to unrealistic spectral shapes that delusive monotonic increase of spectral displacement for longer periods can be detected. Based on high quality strong motion records from different regions (Italy, Greece, Japan, Taiwan), recent research indicates to plausibly shift the cap off period at maximum spectral displacement to adapt for longer-period structures (Bommer and Elnashai 1999, Tolis and Faccioli 1999, Faccioli *et al.* 2004). Eurocode 8 (CEN 2003) indicates to generate the displacement spectrum with a minor change at the prescribed corner period. Higher moment magnitude, M_w=6.9 is selected conservatively, which yields T_D=4.0 s for corner period, based on the formulation $T_D = 1.0 + 2.5 (M_w – 5.7)$ (Faccioli *et al.* 2004). The motive behind the augmentation of corner period is to cover all responses obtained from the selected retrofitting strategies for the structure. If a proposed strengthening induces an increase in the natural period of the structure, the analysis will still be reliable.

Performing nonlinear time-history analyses requires selecting a minimum number of three accelerograms and the most unfavourable response quantity can be regarded as the performance index indicator to represent the overall seismic hazard of a specific site. Alternatively, seven or more seismic records can be employed, and the averaged response quantities are assigned as the performance criteria as recommended in Eurocode 8 (CEN 2003). For the current study, seven ground motions compatible with the design displacement spectrum (tabulated in Table 2 and depicted in Fig. 2) are selected from the Selected Input Motions for displacement-Based Assessment and Design (SIMBAD) database according to the recommendation of the software REXEL-DISP (Smerzini *et al.* 2014). In the software REXEL-DISP, the target spectrum is incorporated

Table 2 Selected ground motions and related characteristics

Rec	Event Name	Country	Station	Date	Magnitude	Dist (km)	PGA (g)
1	Erzincan	Turkey	ERZ	13.03.1992	6.6	8.9	0.50
2	Darfield	N. Zealand	DFHS	03.09.2010	7.0	9.0	0.51
3	Gazli	USSR	KAR	17.05.1976	6.7	12.8	0.72
4	Imperial Valley	US	El C. Val. Irr Dist	19.05.1940	6.9	10.0	0.46
5	Imperial Valley	US	El C. Ar. 5, J. R.	19.05.1940	6.9	4.1	0.49
6	Christchurch	N. Zealand	PRPC	21.02.2011	6.3	6.0	0.67
7	Northridge	US	Rinaldi FF	17.01.1999	6.7	7.5	0.53

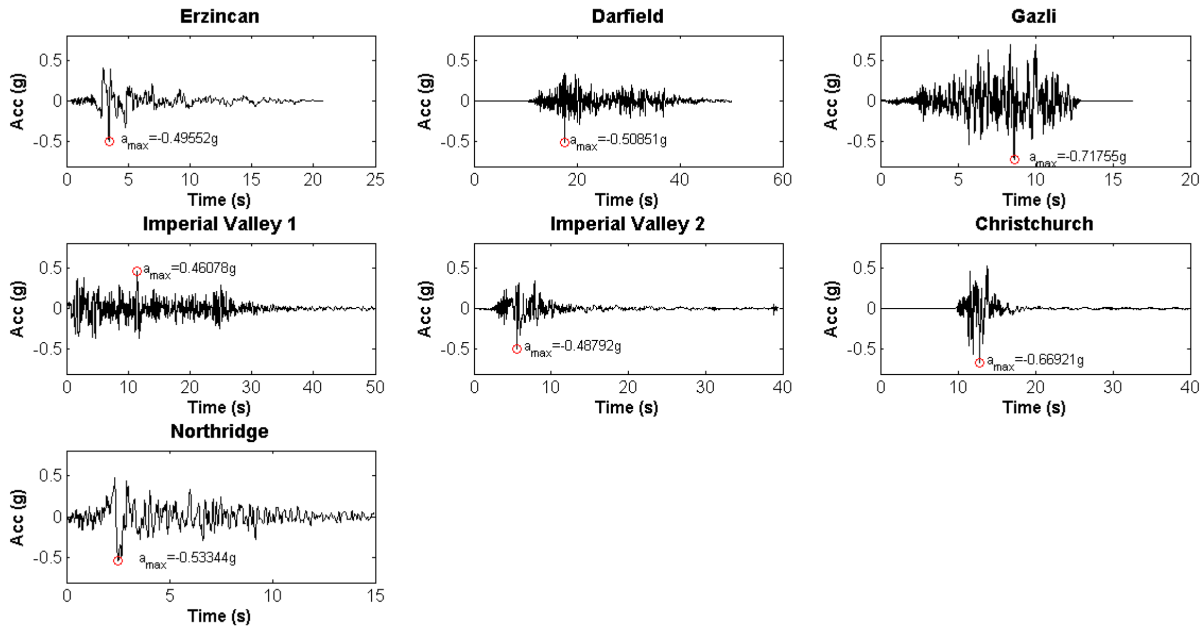

Fig. 2 Acceleration time histories of the selected records

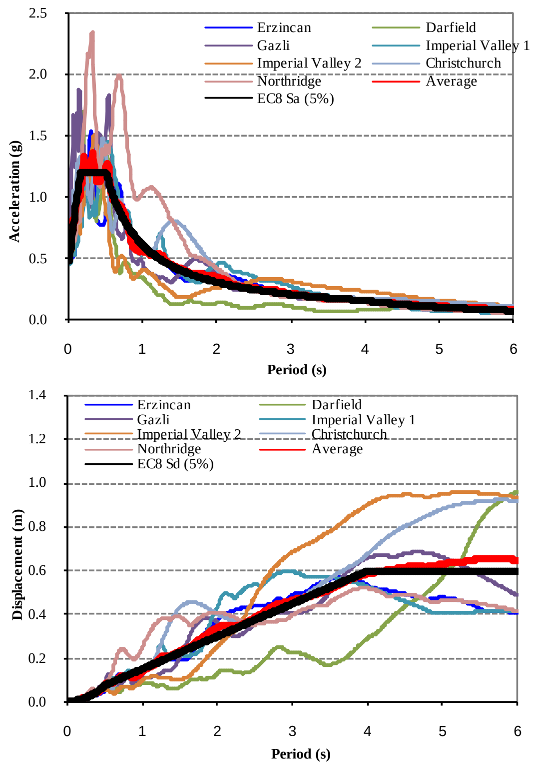

Fig. 3 Acceleration (left) and displacement (right) response spectra for the selected records

by inputting the site class, topographic category, nominal life, functional type, and limit state. The database of SIMBAD is then selected, where the magnitude of earthquake and the distance from the fault source can be defined. Spectrum matching is conducted based on preselected lower and upper tolerances, and ranges of natural period. Displacement and acceleration response spectra of each accelerogram with a shift of corner period to 4 s are derived using the software SeismoSignal (2011) and displayed individually at Fig. 3, which also exhibits the averaged response spectrum along with code specified elastic spectrum at 5% damping level.

3.2 Structural performance level

Performance index, in terms of maximum interstorey drifts, residual interstorey drifts and maximum floor accelerations, can be utilized to identify the deficiencies of the system (SEAOC 1995). This paper follows the recommended performance levels in FEMA-356 (2000). Table 3 presents various maximum interstorey drift ranges. Residual deformation is induced by the inelastic response of the structure, which will be perceivable by occupants if a certain level is exceeded. Recent studies indicate that it may be preferable from an economic point of view to rebuild, rather than retrofit a structure, that has sustained more than

Table 3 Structural performance levels in terms of maximum interstorey drifts (FEMA-356 2000)

Maximum Interstorey Drift	Damage Level
0.0 to 0.5%	Practically no damage
0.5 to 1.0%	Minor damage to non-structural elements
1.0% to 2.0%	Minor to moderate structural damage; Major damage to non-structural elements
2.0% to 4.0%	Major structural damage
Over 4-5%	Potential building collapse

Table 4 Structural performance levels in terms of residual drifts (FEMA-356 2000)

Residual Drift	Damage Level
0.0 to 0.6%	Building is likely usable from an occupant perspective
0.6 to 1.0%	Building likely requires repairs (likely less expensive to demolish and rebuild)
Over 1.0%	Building is structurally unfit to resist another earthquake and could be considered a total loss

0.6% residual drift (Pampanin *et al.* 2002). However, this paper sticks to use the classification of residual drifts defined in FEMA-356 (2000) as illustrated in Table 4. The absolute floor accelerations will result in proportional horizontal inertia forces at each level of a building. Non-structural elements such as furniture, computer and other equipment will be toppled due to large inertia forces. The toppling actions of these elements may lead to severe injuries or even casualties regardless of structural damage levels. Table 5 demonstrates damage levels assigned for absolute horizontal floor accelerations.

3.3 Seismic evaluation

Nonlinear time-history analysis of the structure is to be conducted for three intensity levels of ground motions. The selected seven records fall into the category of design basis earthquake (DBE), which has a probability of exceedance of 10% in 50 years and approximately corresponds to an average return period of 475 years. To represent a frequent earthquake (FE), the accelerogram is scaled down with a factor of 1/2. This earthquake is expected to occur once in approximately 72 years; that is, it has a 50% probability of being exceeded in 50 years. Similarly, the original records are scaled up with a factor of 3/2 to represent a maximum credible earthquake (MCE). MCE level generates a seismic scenario that has a probability of exceedance of 2% in 50 years which is approximately corresponding to an average return period of 2450 years (FEMA-450 2003).

4. Retrofitting strategies

4.1 Retrofit design criteria

The investigated structure needs an urgent retrofit before it faces a DBE or MCE intensity level (will be given in a

Table 5 Structural performance levels in terms of absolute horizontal floor acceleration (FEMA-356 2000)

Absolute Floor Acceleration	Damage Level
0.0 to 0.5 g	Some furniture toppling
0.5 to 1.0 g	Severe accelerations, most furniture toppled over, some damage to sensitive equipment
Over 1.0 g	Interior spaces completely in shambles, severe damage to sensitive equipment

later section). Otherwise, it will be catastrophic and induce economic losses in large scale. The distribution of interstorey drifts should be corresponding to the 1st mode shape. Otherwise, an abrupt change in stiffness exists in the related storey compared to the others. Thus, the proposed rehabilitation should be capable of eliminating uneven stiffness distribution along the building height. Besides, floor accelerations or energy input to the structure must also be limited. This could be accomplished by either adding base isolation device or weakening the structure at specific locations to decrease the overall stiffness. A better response will be obtained if damping is accompanied by the retrofitting schemes (Lavan *et al.* 2008).

Broad ranges of retrofitting scenarios could be applied to the system to upgrade the building to a seismically safe band. The encountered issue at this stage is to select the most effective retrofitting strategy. Many conventional upgrading techniques such as construction of additional shear walls, column jacketing and application of Fiber Reinforced Polymer (FRP) to columns are available (Pinho 2001). These techniques may lead to increased budget of the project since substantial amount of demolition is required which is followed by reconstruction. Besides, these implementations lead to long downtime, during which the occupants should be relocated to other residences. Conventional techniques may end up adding rigidity to the frames, which will attract excessive ground accelerations. Increased floor accelerations cause higher lateral forces acting on structural members and foundation. Hence, these conventional techniques are not considered here for this simple residential building.

Innovative retrofitting technologies such as the implementation of hysteretic, visco-elastic or viscous dampers, the introduction of tuned mass damper, base isolation systems and weakening the structure will be systematically evaluated (Constantinou *et al.* 1998, Di Sarno and Elnashai 2005, Christopoulos and Filiatrault 2006). These applications may require decreased budget, less downtime, less disturbance to the occupants and be relatively easier to implement. Comparative study between various schemes will be presented in the following sections.

4.2 Proposed retrofitting strategies

4.2.1 Hysteretic damper

Chevron-braced frames are introduced in the middle bay of the moment resisting frame (Fig. 4), where hysteretic dampers are installed at one end of the bracing member. Assuming shear type response of the frame, the activation

Table 6 Calculations of shear forces and activity forces for hysteretic dampers

Record	a_g (g)	T_g (s)	T_u (s)	T_b (s)	N_f	W (kN)	V_0 (kN)	V_{ai} (kN)	γ_1 (∘)	$\gamma_{2\text{-}5}$ (∘)	k_1 (kN/mm)	$k_{2\text{-}5}$ (kN/mm)	F_1 (kN)	$F_{2\text{-}5}$ (kN)
1	0.496	0.3	1.067	0.507	5	14192.64	5020.74	502.07	54.58	47.56	272	316	433	372
2	0.509	0.2					3434.89	343.49					296	254
3	0.718	0.14					3391.70	339.17					293	251
4	0.461	0.52					8088.52	808.85					698	599
5	0.488	0.34					5598.40	559.84					483	415
6	0.669	0.46					10383.62	1038.36					896	769
7	0.533	0.4					7193.70	719.37					621	533

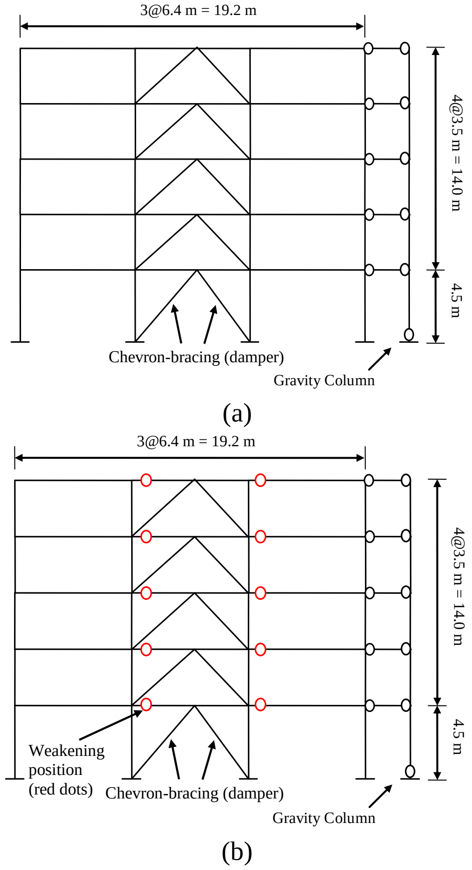

Fig. 4 Diagonally implemented dampers in the frame (a) and weakening the structure (b)

loads of each damper should be in proportional to the interstorey drifts initiated at the first mode vibration of the structure following the optimum hysteretic design spectra method (Filiatrault and Cherry 1990).

$$\frac{V_0}{W} = \frac{a_g}{g} Q\left(\frac{T_b}{T_g}, \frac{T_b}{T_u}, N_f\right) \tag{1}$$

where Q is given as follows

$$Q = \begin{cases} \dfrac{T_g}{T_u}\left[(-1.24N_f - 0.31)\dfrac{T_b}{T_u} + 1.04N_f + 0.43\right] \\ \quad for\ 0 \le T_g / T_u \le 1 \\ \dfrac{T_b}{T_u}\left[(0.01N_f + 0.02)\dfrac{T_g}{T_u} - 1.25N_f - 0.32\right] \\ + \dfrac{T_g}{T_u}(0.02 - 0.002\,N_f) + 1.04N_f + 0.42 \ \text{ for } T_g / T_u > 1 \end{cases} \tag{2}$$

$$F_{ai} = \frac{V_{ai}}{2\cos\gamma_i} \tag{3}$$

$$k_i = \frac{EA}{L_i} \tag{4}$$

where W is the total weight, N_f is the number of storeys, a_g is the peak ground acceleration, T_g is the predominant period of ground motion, T_u and T_b are the fundamental period of the unbraced (original) and the braced structure respectively, V_0 is the total shear force required to active all dampers, γ_i is the inclined angle of the bracing from the horizontal axis, V_{ai} is the optimum distribution of shear forces, Fai is the activation force, E is the Young's modulus, A is the area, L_i is the length and k_i is the stiffness of the bracing. The subscript i represents the floor number.

Table 6 presents the required structural parameters and ground motion characteristics for shear force calculations, from which activation loads of hysteretic damper for every storey can be computed. The braced period of the structure, T_b, is derived in eigenvalue analysis by implementing an assumed section of diagonal bracing to the numerical model as depicted at Fig. 4. These diagonal bracing elements with hysteretic dampers are modeled as bilinear springs that will supply additional stiffness till the yield force (i.e., activation force). Rectangular hollow cold-formed cross sections (EN10219: S355J2H) are selected from British Standard (2006). The bracings of this application are not designed to provide extra stiffness to the structure, while they are simply chosen to install hysteretic dampers. However, it is aware that steel design specifies different classes of cross sections, depending on the occurrence of local and global buckling under bending. Ten trial sections are therefore selected with the increase of the cross-section area and the corresponding activation loads as presented at Table 7.

Ten trial cases are implemented to the building and nonlinear time-history analyses have been performed for seven compatible records at MCE level. The prescribed maximum performance indices are presented at Fig. 5, where the 0-th configuration corresponds to the original structure. The dark horizontal lines envelop the limit states for different indices. Before rehabilitation, maximum and residual interstorey drifts could induce major damage to the structure. Maximum floor accelerations were far beyond 1.0 g limit state, over which severe damage to all private properties can be expected and it may cause casualties. As an interpretation of retrofit results, one can infer that considerable improvements are achieved by introducing hysteretic dampers. In general, the building shows

Table 7 Selection of trial bracing sections

Configuration	Selected section	Area (mm^2)	k_1 (kN/mm)	$k_{2\text{-}5}$ (kN/mm)	T_b/T_u	F_1 (kN)	$F_{2\text{-}5}$ (kN)
1	W140×80×6.3	2480	90	105	0.639	518	445
2	W250×100×8	5120	181	211	0.533	762	654
3	W200×100×12.5	6200	225	261	0.503	832	714
4	W250×100×12.5	7450	272	316	0.475	896	769
5	W300×200×10	9260	335	391	0.450	954	819
6	W350×250×11	12500	453	527	0.415	1035	889
7	W350×250×12	13200	478	557	0.409	1048	900
8	W300×200×16	13900	507	590	0.403	1063	913
9	W400×300×12	15600	565	658	0.391	1088	935
10	W400×200×16	17100	634	738	0.380	1114	957

Table 8 Trial cases to capture the effects of various viscous damping coefficients

Parameter	Case 1	Case 2	Case 3	Case 4	Case 5
Fundamental period of the unbraced fame T_1 (s)	1.067	1.067	1.067	1.067	1.067
Inherent damping of the structure, ξ_{in} (%)	5	5	5	5	5
Targeted damping by viscous damper, ξ_d (%)	10	15	20	25	30
Desired viscous damping, ξ_1 (%)	15	20	25	30	35
Required fundamental period, $\hat{T}_1$ (s)	0.936	0.902	0.871	0.844	0.818
Fictitious fundamental period, $\hat{T}_{1tr}$ (s)	0.792	0.792	0.792	0.792	0.792

Table 9 Calculated initial interstorey stiffness, fictitious spring constants and linear viscous damper constants for trial cases

Storey	Initial stiffness $\hat{k}_{0tr}$ (kN/mm)	Case 1		Case 2		Case 3		Case 4		Case 5	
		$\hat{k}_0$	C_L (kN·s/mm)	$\hat{k}_0$	C_L (kN·s/mm)	$\hat{k}_0$	C_L (kN·s/mm)	$\hat{k}_0$	C_L (kN·s/mm)	$\hat{k}_0$	C_L (kN·s/mm)
5	21.64	11.12	1.89	13.76	2.34	16.06	5	21.64	11.12	1.89	13.76
4	34.50	17.73	3.01	21.95	3.73	25.60	4	34.50	17.73	3.01	21.95
3	51.58	26.50	4.50	32.81	5.57	38.28	3	51.58	26.50	4.50	32.81
2	73.88	37.96	6.45	46.99	7.98	54.83	2	73.88	37.96	6.45	46.99
1	112.01	57.55	9.77	71.25	12.10	83.12	1	112.01	57.55	9.77	71.25

improved performance when a damper with larger sectional area or stiffness is implemented, but small fluctuations of the performance can be observed. However, there is a trade-off between the effectiveness of hysteretic dampers and the cost availability of material (i.e., selection of diagonal bracings).

4.2.2 Linear viscous damper

Viscous-type energy dissipating devices can be instead assembled at one end of the bracing member, Fig. 4. The damping force is out of phase with the displacement demand. In other words, this damper generates zero and maximum forces to the lateral system at maximum and zero drifts, respectively, during earthquakes. Based on modal superposition, a convenient trial-and-error design process is favoured in most practical design practices (Christopoulos and Filiatrault 2006).

$$\xi_1 = \xi_{in} + \xi_d \tag{5}$$

$$\hat{T}_1 = \frac{T_1}{\sqrt{2\xi_1 + 1}} \tag{6}$$

$$\hat{k}_0 = \frac{\hat{k}_{0tr}}{1 - \left(\dfrac{\hat{T}_1^2 - \hat{T}_{1tr}^2}{\hat{T}_1^2 - T_1^2} \right)} \tag{7}$$

$$C_L = \frac{T_1}{2\pi} \hat{k}_0 \tag{8}$$

where ξ_{in} and ξ_d are the inherent damping of the structure and the designed damping induced by viscous damper, respectively. The total damping ξ_1 can be used to calculate the required fundamental period $\hat{T}_1$ from the natural period of the original configuration, T_1. $\hat{k}_{0tr}$ is the initial trial stiffness coefficient of the fictitious springs. The trial fundamental period of the fictitious braced structure $\hat{T}_{1tr}$ can be evaluated from eigenvalue analysis of the braced model using the initial trial stiffness. $\hat{k}_0$ denotes the additional stiffness of the chevron bracing. C_L represents the damping constant of viscous dampers.

Numerical parametric analyses can be performed using the computed values as tabulated in Tables 8 and 9. The responses of both the original and rehabilitated structures at

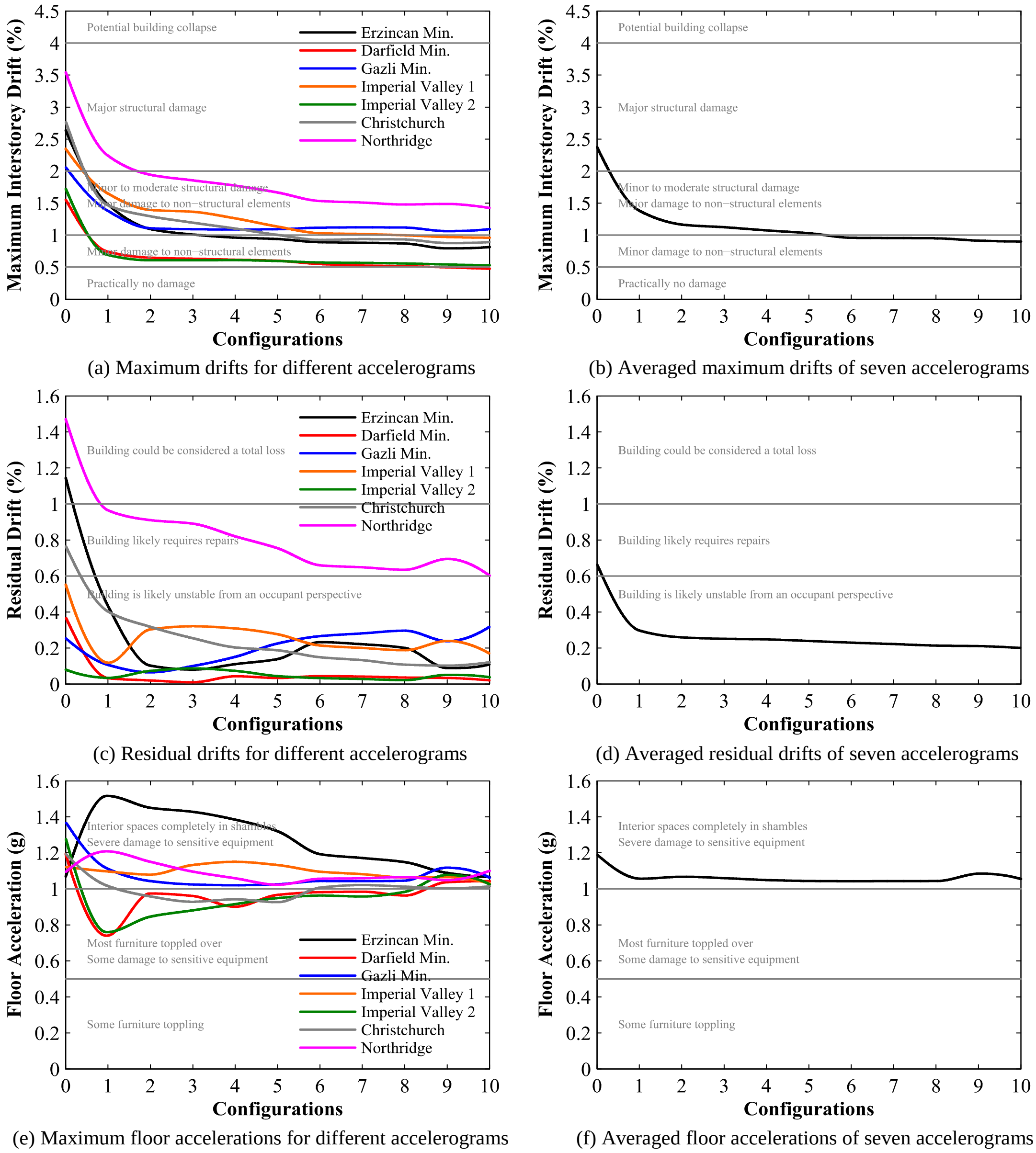

(a) Maximum drifts for different accelerograms

(b) Averaged maximum drifts of seven accelerograms

(c) Residual drifts for different accelerograms

(d) Averaged residual drifts of seven accelerograms

(e) Maximum floor accelerations for different accelerograms

(f) Averaged floor accelerations of seven accelerograms

Fig. 5 Results obtained from different configurations for hysteretic dampers

MCE hazard level are compared in Fig. 6. For the 0-th configuration case, values obtained from the initial building are presented, and the efficiency of retrofitting schemes for other scenarios can be perceived accordingly. The maximum and residual interstorey drifts drop substantially to minor structural damage level due to induced damping. As expected, improved results are obtained as the viscous damping increases from the configuration 1 to 5. However, linear viscous dampers cannot control the maximum floor accelerations, which tend to be higher than in the case of the original building.

4.2.3 Base isolation

The option of retrofitting the building with Friction Pendulum (FP) isolated bearings is considered in this section. A base isolated structure is supported by a series of bearing pads, which are placed between the building and its foundation. Such friction-type sliding bearings use gravity as the restoring force. They can be directly installed under the vertical load bearing members or they can be situated under a new casted foundation that acts as a diaphragm at ground floor level. The number of bearings should be minimized to ensure a lower cost. Wind loads could govern the design, and enough static frictional forces must be supplied by the bearings to prevent its activation under lateral pressures. An optimal allocation of bearings needs to be determined in accordance with the initial configuration of the structure. In the numerical model, the horizontal constraints under moment resisting frame are set free, and they are then restrained to the most left node at the ground level, which is attached to a newly created fixed node via spring (corresponding to rollers that will illustrate the behaviour of friction pendulum isolation system – bearing pads). This spring has less lateral stiffness compared to the lateral stiffness of the structure. As the lateral stiffness of the system is reduced at the location of input acceleration,

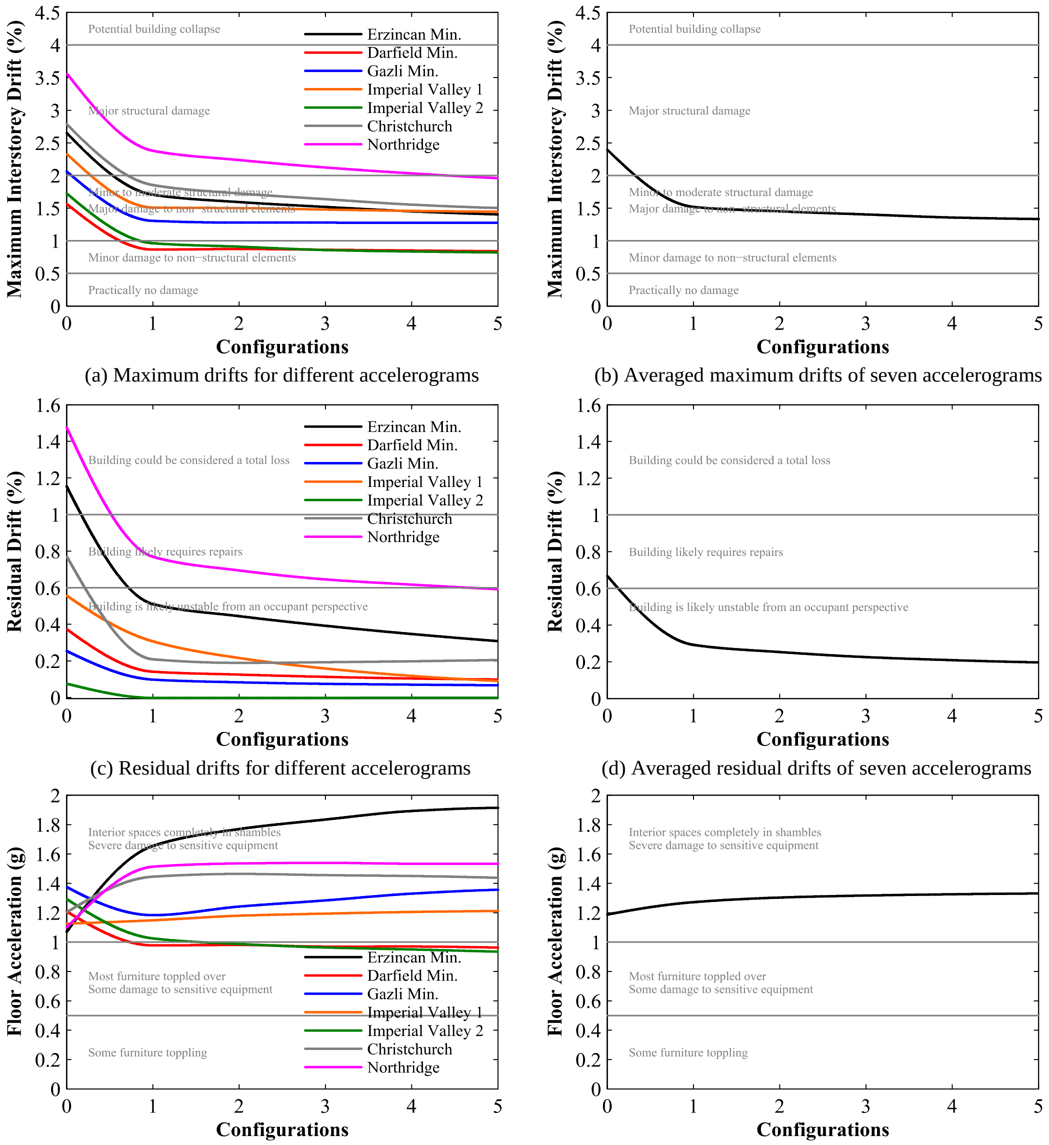

(a) Maximum drifts for different accelerograms (b) Averaged maximum drifts of seven accelerograms

(c) Residual drifts for different accelerograms (d) Averaged residual drifts of seven accelerograms

(e) Maximum floor accelerations for different accelerograms (f) Averaged floor accelerations of seven accelerograms

Fig. 6 Results obtained from different configurations for linear viscous dampers

most of the deformations (mainly lateral rigid body motion) are concentrated on bearings.

For the preliminary design, the Single Curvature FP (SCFP) system is selected, which consists of an articulated slider and a spherical concave base plate. The uplift of slider is controlled by the radius of concave lining surface. It only permits a sliding of 300 mm on the bottom plate. This is due consideration of economic issues that a higher displacement capacity of the isolator (exceeds 300 mm) indicates a bigger radius of FP and corresponding exponentially increased cost. This building contains two exterior moment resisting frames, under which the bearings should be installed (8 bearings, n_b and 12 rollers, n_r). The isolator bearings must be capable of resisting wind loads (Christopoulos and Filiatrault 2006).

$$\mu_s W_b > F_{wind} \tag{9}$$

where μ_s is the coefficient of friction, W_b is the total vertical load on bearings and F_{wind} is the total wind force on the structure, which can be evaluated by the product between the wind pressure (assuming 0.5 kPa in this case) and the facade that is exposed to the wind.

The radius of the FP system (R) is assumed as 3000 mm and the maximum displacement ($D_{\max}$) of the isolator is set to be 250 mm that is lower than 300 mm. The dynamic friction coefficient, μ_d, is set to be equal to static friction of coefficient, μ_s, of 0.04. The total weight on the bearings can be calculated from the total weight of the building (W_t) as follows

$$W_b = \frac{W_t}{n_b + n_r} n_b \tag{10}$$

The effective stiffness, K_{eff}, can be calculated

$$K_{eff} = W_b\left(\frac{1}{R} + \frac{\mu_d}{D_{\max}}\right) \tag{11}$$

The target time period, T_D, and the effective damping

Table 10 Loading cases of optimization criteria to tune the TMD vibration (Constantinou *et al.* 1998)

Loading case	Optimization criteria	Optimum tuning conditions	
		f	c/c_c
Harmonic load applied to primary structure	Minimum relative displacement amplitude of primary structure	$\frac{1}{1+\mu}$	$\sqrt{\frac{3\mu}{8(1+\mu)^3}}$
Harmonic load applied to primary structure	Minimum relative acceleration amplitude of primary structure	$\frac{1}{\sqrt{1+\mu}}$	$\sqrt{\frac{3\mu}{8\left(1+\frac{\mu}{2}\right)}}$
Harmonic base acceleration	Minimum absolute acceleration amplitude of primary structure	$\frac{1}{1+\mu}$	$\sqrt{\frac{3\mu}{8(1+\mu)}}$
Random base acceleration	Minimum root mean square value of relative displacement of primary structure	$\frac{\sqrt{1-\frac{\mu}{2}}}{1+\mu}$	$\sqrt{\frac{\mu\left(1-\frac{\mu}{4}\right)}{4(1+\mu)\left(1-\frac{\mu}{2}\right)}}$

ratio, ξ, are calculated by

$$T_D = 2\pi\sqrt{\frac{W_t}{K_{eff}\,g}} \tag{12}$$

$$\xi = \frac{1}{2\pi}\frac{A_{loop}}{K_{eff}D_{\max}^{2}} = \frac{1}{2\pi}\frac{4D_{\max}\mu_d W_b}{K_{eff}D_{\max}^{2}} = \frac{2\mu_d W_b}{\pi K_{eff}D_{\max}} \tag{13}$$

With the obtained effective damping ratio and period of vibration, the displacement response spectra at Fig. 3 can be utilized to interpret the displacement demand, D_d. The iterative process reaches convergence when there is no significant change in displacement (D_d=$D_{\max}$).

For R=3000 mm, the converged $D_{\max}$ is achieved as 404 mm (with T_D=4.82 s) which is beyond the limit that SCFR can supply (300 mm). Time-history analysis of the system yields the displacement demand of 417 mm. Subsequently, trails of using different radius (R) values are conducted, but none of them provides satisfactory results. Thus, design is shifted to the Double Curvature FP (DCFP) system, which can double the displacement capacity. The same procedure for SCFP is followed with an upgrade at stiffness (K_{eff}) (Constantinou 2004)

$$K_{eff} = W_b\left(\frac{1}{2(R-h)} + \frac{\mu_d}{D_{\max}}\right) \tag{14}$$

where h=100 mm, represents the distance from the spherical concave sliding interfaces and an articulated double friction slider. In this case, the same properties and dimension of the top and bottom plates are assumed. The optimal solution is obtained for R=1250 mm, and $D_{\max}$=277.8 mm.

4.2.4 Tuned mass damper

Tuned mass damper (TMD) or vibration absorber is a relatively small mass spring-dashpot system that is calibrated to be in resonance with a particular mode of a structure. In the current study, this multiple degree of freedom building is transformed into an equivalent single degree of freedom system, from which the fundamental period is determined to indicate the vibrating frequency and the required mass for the damper. This assumption is valid since the performance of the as-built structure is dominated by the first mode at the natural period of 1.067 s with 87% participating masses. A tuned mass damper with less than 10% mass ratio (ratio of the mass of the damper to the mass of the structure) is seen to be more effective than a larger damper (Rildova and Singh 2006). Besides, if the TMD mass is larger than 30% of the primary structure, it will not be economic. Generally, a mass ratio of 2-3% is utilized. The reason for limiting the mass ratio is due to the fact that an increase in the tuned mass leads to additional forces in structural members (Constantinou *et al.* 1998). In this paper, parametric analyses of mass ratio varying between 2-5% are performed to get the optimized solution for this low-rise residential building.

Four different optimization criteria to tune the TMD vibrating with the first mode of the primary structure are used, Table 10. Taking the loading case of harmonic base acceleration as an example, a mass ratio μ of 5% indicates the natural frequency ratio of the primary structure with TMD, f, can be calculated as 0.952. Subsequently, the natural frequency of TMD, ω_a, is obtained as 4.188 rad/s. It also provides the damping ratio, c/c_c, as 0.134. The critical viscous damping constant of TMD, c_c, yields as 0.661 kN·s/mm. The TMD can be simplified as a viscoelastic damper with added weight that is sitting on the roof of the structure. The damping constant, stiffness and added weight of viscoelastic damper are then estimated as 0.0905 kN·s/mm, 1.55 kN/mm and 723.7 kN, respectively. The most effective implementation is to tune the TMD based on the loading case of white noise (random) vibrations with a mass ratio of 2.5% as given in Fig 7.

4.2.5 Weakening and damping technique

Another retrofit strategy considered in the present study is the weakening and damping technique. The structure at selected locations is weakened by strategically releasing the moments at the beam ends (e.g., releasing bolts, removing the complete penetration welds, removing the slab around columns, and removing the cover plate in beams/columns, etc.). The weakening of inelastic structure helps in limiting the experienced maximum accelerations induced by ground motions. But this modification leads to an increase in displacement demands (maximum and residual interstorey drifts). Chevron-braced frames are then installed to add either hysteretic or viscous dampers, which could reduce

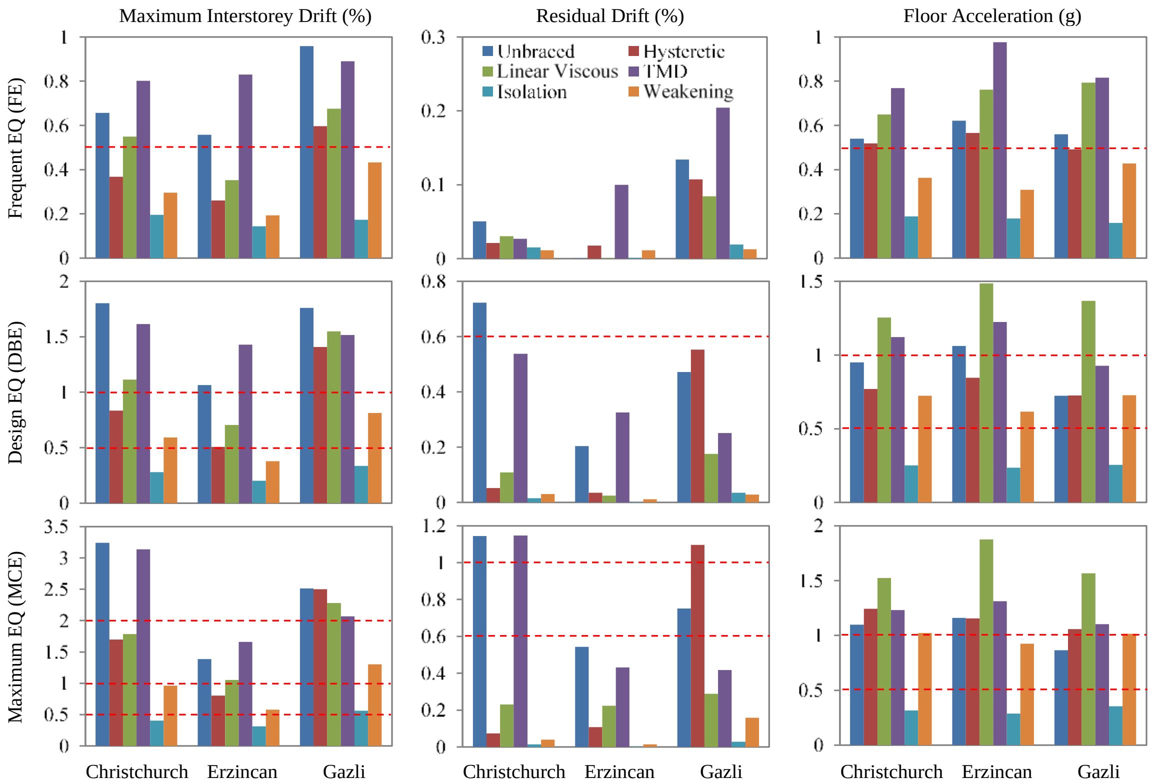

Fig. 7 Comparison of various retrofit strategies (taking 3 records for example)

the interstorey drifts without introducing significant total accelerations. The adopted weakening strategy is shown in Fig. 4 to diminish soft storey effect of the building. Furthermore, the same stiffness of bracing is chosen as 100 kN/mm and a larger damping constant of 20 kN·s/mm is selected at lower stories (1^{st} and 2^{nd}), comparing with 15 kN·s/mm at higher stories.

4.3 Comparison of different retrofit strategies

For brevity, the seismic responses of only three earthquake excitations are presented in Fig. 7. The calculated results of all retrofitted systems are compared against the one evaluated from the original configuration. Various aspects are considered for these retrofit techniques as shown in Table 11. Each one has some benefits over the other and there is a trade-off between various factors to get an optimal solution.

Passive control devices, such as hysteretic and linear viscous dampers, dissipate seismic energy by yielding, friction, or viscosity of the material. These devices stiffen the building and hence reduce the interstorey drifts. However, they are not capable of reducing the floor accelerations, in particular in those storeys undergoing inelastic deformations. Moreover, an increase in accelerations could happen due to additional stiffnesses induced by these dampers. For hysteretic damper, the floor acceleration is increased by 13% and 22% for Christchurch and Gazli earthquakes under MCE level, respectively. The acceleration response is even worse for linear viscous damper that 39%, 62% and 81% increased accelerations are obtained for Christchurch, Erzincan and Gazli earthquakes at MCE level correspondingly. The implementation may also lead to a substantial increase in maximum base shear and column axial forces, such that strengthening of the columns and foundation is often required in practice.

Base isolation is found to be the best technique that can limit all the performances (maximum and residual interstorey drifts and floor accelerations) within desired levels for various earthquakes at three intensity levels. This technique could be beneficial in long-term, but it is highly expensive as for capital costs in short-term. Sometimes, the occupants have to be evacuated for a while, even though the building can be lifted up in some cases with no disturbance to occupants. Also it requires the construction of a new link frame for the entire building, which demands highly skilled construction techniques and advanced technologies. Although this technique yields good results, it is not advised from the economic, intervention and implementation point of view.

The performance of tuned mass damper is not satisfactory, as it leads to a slightly increase in structural responses compared to the original configuration at frequent earthquake level (e.g., the maximum interstorey drift is increased by 22% and the floor acceleration is increased by 42% for Christchurch earthquake) and a reduced seismic demands at DBE (e.g., the maximum interstorey drift is decreased by 14% and the residual drift is decreased by 47% for Gazli earthquake) and MCE levels (e.g., the maximum interstorey drift is decreased by 44% and the residual drift is decreased by 18% for Gazli earthquake). One can expect that a FE level earthquake is not strong enough to activate the damper and the added mass deteriorates the performance of the structure, which is

Table 11 Comparisons of various retrofit strategies

Benefit factors		Hysteretic	Viscous	Base Isolation	Tuned mass damper	Weakening+ Dampers
Implementation/Construction		*Easy*	*Easy*	*Difficult* (Needs skilled labour and advanced technologies)	*Extra* room is required at the top of the building	Easy (be carried out without much effort)
Disturbance to occupants and downtime		*Less*	*Less*	Building has to be *evacuated* till retrofitting got over	Almost *negligible* disturbance as the construction is at the new floor	Comparatively *less*
Additional retrofitting needed for beam/columns due to the extra force caused due to retrofitting		*High* as the dampers add more stiffness to the building and attracts more force	Attracts *extra* force to the members	Very *less* as the base isolation prevents the transmission of force to the superstructure	*Extra load* from the addition mass on all the columns	Weakening causes *less force* attraction as the flexibility of building increases with weakening
Performance compared to un-braced frame (original building)	*Interstorey drift*	Reduces	Reduces	Very less	Higher	Less
	Residual drift	Reduces	Reduces	Almost negligible	Higher	Less
	Floor acceleration	Higher	Higher	Very less	Higher	Less
Intervention to foundation because of the additional force on members due to retrofitting		*Yes*, to include the additional force	*Yes*, to include the additional force	*Maximum*, as extra link frame is needed	*Yes*, to include the additional mass on top (if extra mass is less than 5% then less intervention)	*Less*, as weakening causes a reduction of force
Cost of retrofitting		Less	Less	Very High	Less	Less
Aesthetics		Extra chevron braces looks *bad*	Extra chevron braces looks *bad*	Will *not* be affected	Will *not* be affected	Extra chevron braces looks *bad*

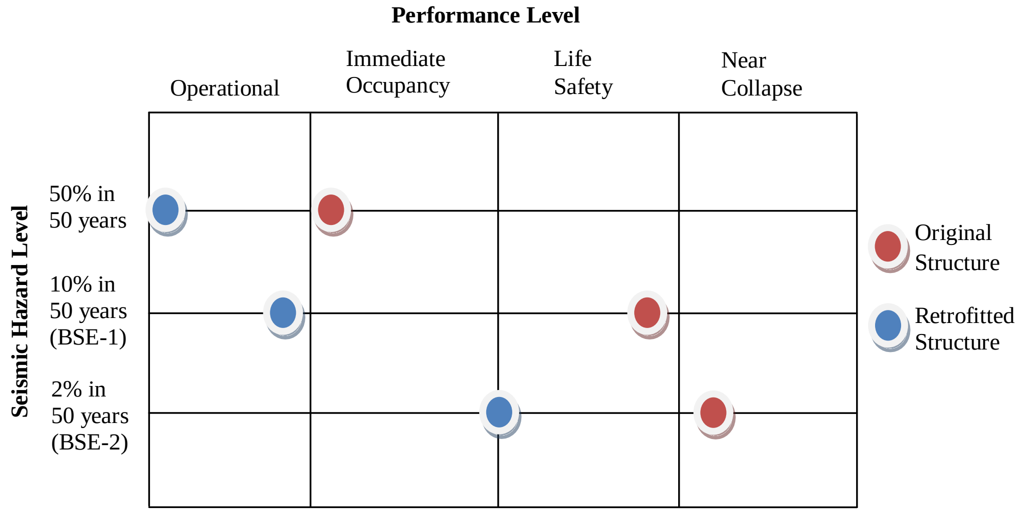

Fig. 8 Modification of performance levels by weakening and damping technique

improved as the earthquake intensity increases to DBE and MCE levels. However, floor acceleration is a major issue for this retrofitting scheme, since additional structure on top of the building can attract more seismic energy. The deficiency of TMD in this application may be related to the simple design procedure and the soft storey effect of the initial building. Besides, this type of damper is normally applied in high-rise buildings. For this simple five-storeys building, it would not be cost effective. No further investigation has been done on this damper.

In this case study, the weakening and damping technique seems to be the optimal solution considering all factors including cost, downtime, easiness in implementation and disturbance to the occupants. More stiffness the structure has, more horizontal accelerations the floors attract. Weakening could potentially reduce the maximum floor accelerations (e.g., the acceleration is decreased by 50%, 42% and 20% for Erzincan earthquake at FE, DBE and MCE levels, respectively), but at the same time, induce more interstorey drifts. On the other hand, dampers provide energy dissipation through yielding, friction, or viscosity of the material, which helps in limiting these drifts (e.g., the maximum interstorey drift is decreased by 55%, 67% and 70% for Christchurch earthquake at FE, DBE and MCE levels, respectively and the residual drift is decreased by 90%, 94% and 79% for Gazli earthquake at FE, DBE and MCE levels, respectively). Both structural and non-structural damages in the building can be prevented.

Table 12 Seismic performance of moment-resisting steel framed building in terms of engineering response indices (FEMA-356 2000)

Performance Level	Description of Structural Damage	Maximum Drift	Residual Drift
Collapse Prevention	Extensive distortion of beams and column panels; many fractures at moment connections, but shear connections remain intact.	5%	5%
Life Safety	Plastic hinges form; local buckling of some beam elements; severe joint distortion; isolated connection and element fractures, but shear connections remain intact.	2.5%	1%
Immediate Occupancy	Minor local yielding at a few locations; no fractures; minor buckling or observable permanent distortion of members.	0.7%	-

4.4 Performance of the suggested optimal retrofit

The improvement in performance levels (Table 12) obtained from the building rehabilitated by the selected optimal retrofit option of the weakening and damping (visco-elastic dampers) technique can be seen in Fig. 8. At FE hazard level, the retrofit helps in improving the performance from “Immediate Occupancy” to “Operational” level. A tremendous change in performance from “Life safety” to “Operational” can be achieved with the retrofit at DBE hazard level. For the MCE hazard level, the retrofit strategy moves the performance level from “Near Collapse” to “Immediate Occupancy”.

5. Conclusions

Selection of the most suitable retrofit strategy for a building is not straightforward, as there is no alternative which clearly emerges among others as the best one according to the whole criteria considered (i.e., cost, downtime, implementation, etc.). A trade-off between various parameters has to be taken into account to derive the final retrofit strategy. The structure can be made much stiffer by adding extra elements (i.e., shear walls) to enable it to behave in the linear elastic range during earthquakes. This could be effective in reducing displacement demands, but detrimental to floor accelerations of the structure. In addition, the overall cost of such rehabilitation may be almost equal or even higher than demolishing and constructing a new building. The basic idea is to limit the displacement and acceleration demands at the same time.

In this paper, a simple five-storeys steel residential building is analyzed and retrofitted with various schemes. Comparative study shows that hysteretic damper generally leads to an increase in floor acceleration by at least 10% and substantial augment of floor acceleration by approximately 40% could be obtained for linear viscous damper. Base isolation system provides the best solution, but it is not recommended due to construction efforts. Tuned mass damper can effectively reduce the structural responses at DBE or MCE levels, but not efficient at FE level, where the response is worsened by as high as 20%. The rehabilitation strategy, consisting of weakening the structure and adding additional damping devices, is finally recommended as the optimal solution. The proposed procedure modifies both the floor accelerations and drifts to enhance the structural performance from at-risk level to safety level. The weakening technique alone could decrease inelastic floor accelerations by at least 20% and thus base shears, but increase ductility demands. Introducing structural damping alone produces a strong reduction in ductility demands (reducing drifts by more than 50%), without much improvement of accelerations. The combined retrofit reduces all responses depending on the amount of strength reduction and added damping. However, it must be emphasized that the benefits of this procedure have to be restrained to this special structure case. For a general regulation, case-by-case analysis has to be performed prior to implementation of any upgrading procedure.

References

Bommer, J.J. and Elnashai, A.S. (1999), “Displacement spectra for seismic design”, *J. Earthq. Eng.*, **3**(1), 1-32.

British Standards (2006), Cold Formed Welded Structural Hollow Sections of Non-alloy and Fine Grain Steels, EN- 10219-1, BSI, London, UK.

Calvi, G.M. and Kingsley, G.R. (1995), “Displacement based seismic design of multi-degree of freedom bridge structures”, *Earthq. Eng. Struct. Dyn.*, **24**(9), 1247-1266.

Calvi, G.M. and Sullivan, T.J. (2009), *A Model Code for the Displacement-based Design of Structures*, IUSS Press, Pavia, Italy.

Cardone, D., Perrone, G. and Sofia, S. (2011), “A performance-based adaptive methodology for the seismic evaluation of multi-span simply supported deck bridges”, *Bull. Earthq. Eng.*, **9**(5), 1463-1498.

Carr, A.J. (2005), “Ruaumoko2D: Time history analysis of non-linear two-dimensional structures, and Post-processor for Ruaumoko: Dynaplot, User manual”, Computer Program Library, Department of Civil Engineering, University of Canterbury, Christchurch, New Zealand.

CEN (2002), Eurocode 1: Actions on structures-Part 1-1: General actions-Densities, self-weight, imposed loads for buildings, EN 1991-1-1, Comité Européen de Normalisation, Brussels, Belgium.

CEN (2003), Eurocode 8: Design of structures for earthquake resistance-Part 1: General rules, seismic actions and rules for buildings, prEN 1998-1, Comité Européen de Normalisation, Brussels, Belgium.

Christopoulos, C. and Filiatrault, A. (2006), *Principles of Passive Supplemental Damping and Seismic Isolation*, IUSS Press, Pavia, Italy.

Ciampoli, M. and Pinto, P.E. (1995), “Effects of soil-structure interaction on inelastic seismic response of bridge piers”, *J. Struct. Eng.*, **121**(5), 806-814.

Cimellaro, G.P., Lavan, O. and Reinhorn, A.M. (2009), “Design of passive systems for control of inelastic structures”, *Earthq. Eng.*

Struct. Dyn., **38**(6), 783-804.
Constantinou, M.C. (2004), "Friction pendulum double concave bearing", Technical Report, University at Buffalo, State University of New York, Buffalo, NY.
Constantinou, M.C., Soong, T.T. and Dargush, G.F. (1998), "Passive energy dissipation systems for structural design and retrofit", MCEER-98-MN01, Multidisciplinary centre for earthquake engineering research, University of Buffalo, Buffalo, New York, U.S.
Della Corte, G., De Risi, R. and Di Sarno, L. (2013), "Approximate method for transverse response analysis of partially isolated bridges", *J. Bridge Eng.*, **18**(11), 1121-1130.
Dhakal, R.P., Mander, J.B. and Mashiko N. (2006), "Identification of critical ground motions for seismic performance assessment of structures", *Earthq. Eng. Struct. Dyn.*, **35**(8), 989-1008.
Di Sarno, L. and Elnashai, A.S. (2003), "Special metals for seismic retrofitting of steel buildings", *Prog. Struct. Eng. Mater.*, **5**(2), 60-76.
Di Sarno, L. and Elnashai, A.S. (2005), "Innovative strategies for seismic retrofitting of steel and composite structures", *Prog. Struct. Eng. Mater.*, **7**(3), 115-135.
Di Sarno, L. and Elnashai, A.S. (2009), "Bracing systems for seismic retrofitting of steel frames", *J. Constr. Steel Res.*, **65**(2), 452-465.
Di Sarno, L. and Manfredi, G. (2012), "Experimental tests on full-scale RC unretrofitted frame and retrofitted with buckling-restrained braces", *Earthq. Eng. Struct. Dyn.*, **41**(2), 315-333.
Elenas, A. and Vasiliadis, L. (2002), "Retrofit of a stone masonry school building damaged during the Athens earthquake of 7 September 1999", *Proceedings of 12th European Conference on Earthquake Engineering*, London, UK, September.
Elnashai, A.S. and Di Sarno, L. (2008), *Fundamentals of Earthquake Engineering*, Wiley, New York.
El-Tawil, S., Vidarsson, E., Mikesell, T. and Kunnath, S.K. (1999), "Inelastic behavior and design of steel panel zones", *J. Struct. Eng.*, **125**(2), 183-193.
Faccioli, E., Paolucci, R. and Rey, J. (2004), "Displacement spectra for long periods", *Earthq. Spectra*, **20**(2), 347-376.
Faella, C., Martinelli, E. and Nigro, E. (2004), "Seismic assessment and retrofitting of r.c. existing buildings", *Proceedings of 13th World Conference on Earthquake Engineering*, Vancouver, B.C., Canada, August.
Fardis, M. (2007), "Guidelines for displacement-based design of buildings and bridges (LESSLOSS Report-2007/05)", IUSS Press, Pavia, Italy.
FEMA-356 (2000), Prestandard and Commentary for the Seismic Rehabilitation of Buildings, Federal Emergency Management Agency, Washington, DC.
FEMA-450 (2003), NEHRP Recommended Provisions for Seismic Regulations for New Buildings and Other Structures, Federal Emergency Management Agency, Washington, DC.
Filiatrault, A. and Cherry, S. (1990), "Seismic design spectra for friction damped structures", *J. Struct. Eng.*, **116**(5), 1334-1355.
Ghobarah, A. and Abou-Elfath, H. (2001), "Rehabilitation of a reinforced concrete frame using eccentric steel bracing", *Eng. Struct.*, **23**(7), 745-755.
Griffith, M. (2008), "Seismic retrofit of RC frame buildings with masonry infill walls: literature review and preliminary case study", JRC Scientific and Technical Reports, The Institute for the Protection and the Security of the Citizen, Ispra, Italy.
Kim, J., Choi, H. and Min, K.W. (2003), "Performance-based design of added viscous dampers using capacity spectrum method", *J. Earthq. Eng.*, **7**(1), 1-24.
Kim, K.D. and Engelhardt, M.D. (2002), "Monotonic and cyclic loading models for panel zones in steel moment frames", *J. Constr. Steel Res.*, **58**(5), 605-635.
Kowalsky, M.J., Priestley, M.J.N. and MacRae, G.A. (1995), "Displacement-based design of RC bridge columns in seismic regions", *Earthq. Eng. Struct. Dyn.*, **24**(12), 1623-1643.
Krawinkler, H. and Mohasseb, S. (1987), "Effects of panel zone deformations on seismic response", *J. Constr. Steel Res.*, **8**, 233-250.
Lavan, O., Cimellaro, G.P. and Reinhorn, A.M. (2008), "Noniterative optimization procedure for seismic weakening and damping of inelastic structures", *J. Struct. Eng.*, **134**(10), 1638-1648.
Mangalathu, S. and Burton, H. (2018), "Machine learning based damage detection of residential buildings", *Proceedings of Neural Information Processing Systems 2018 (NeurIPS 2018)*, Montreal, Canada.
Mangalathu, S. and Jeon, J.S. (2018), "Classification of failure mode and prediction of shear strength for reinforced concrete beam-column joints using machine learning techniques", *Eng. Struct.*, **160**, 85-94.
Martínez-Rodrigo, M.D. and Filiatrault, A. (2015), "A case study on the application of passive control and seismic isolation techniques to cable-stayed bridges: A comparative investigation through non-linear dynamic analyses", *Eng. Struct.*, **99**, 232-252.
Mylonakis, G. and Gazetas, G. (2000), "Seismic soil-structure interaction: beneficial or detrimental?", *J. Earthq. Eng.*, **4**(3), 277-301.
Ni, P. (2012), "Non-linear dynamic soil-structure interaction for displacement-based seismic assessment of bridges", Master's Thesis, European School for Advanced Studies in Reduction of Seismic Risk (ROSE School), Pavia, Italy.
Ni, P. (2013), "Effects of soil-structure interaction on direct displacement-based assessment procedure of multi-span reinforced concrete bridges", *Eur. J. Environ. Civil Eng.*, **17**(7), 507-531.
Ni, P. (2014), "Seismic assessment and retrofitting of existing structure based on nonlinear static analysis", *Struct. Eng. Mech*., **49**(5), 631-644.
Ni, P. and Mangalathu, S. (2018), "Fragility analysis of gray iron pipelines subjected to tunneling induced ground settlement", *Tunn. Undergr. Sp. Tech.*, **76**, 133-144.
Ni, P., Mangalathu, S. and Liu, K. (2018), "Enhanced fragility analysis of buried pipelines through Lasso regression", *Acta Geotech.*, doi: 10.1007/s11440-018-0719-5.
Ni, P., Mangalathu, S. and Yi, Y. (2018), "Fragility analysis of continuous pipelines subject to transverse permanent ground deformation", *Soils Found.*, **58**(6), 1400-1413.
Ni, P., Petrini, L. and Paolucci, R. (2014), "Direct displacement-based assessment with nonlinear soil-structure interaction for multi-span reinforced concrete bridges", *Struct. Infrastr. Eng.*, **10**(9), 1211-1227.
Ni, P., Wang, S., Jiang, L. and Huang, R. (2012), "Seismic risk assessment of structures using multiple stripe analysis", *Appl. Mech. Mater.*, **226**, 897-900.
Pampanin, S., Christopoulos, C. and Priestley, M.J.N. (2002), "Residual deformations in the performance-based seismic assessment of frame structures", ROSE Research Report 2002/02, IUSS Press, Pavia, Italy.
Panagiotakos, T.B. and Fardis, M.N. (2001), "A displacement-based seismic design procedure for RC buildings and comparison with EC8", *Earthq. Eng. Struct. Dyn.*, **30**(10), 1439-1462.
Paolucci, R., Figini, R. and Petrini, L. (2013), "Introducing dynamic nonlinear soil-foundation-structure interaction effects in displacement-based seismic design", *Earthq. Spectra*, **29**(2), 475-496.
Pinho, R. (2001), "Seismic assessment and upgrading of reinforced concrete buildings", *Proceedings of 20th European Regional Earthquake Engineering Seminar*, Sion, Switzerland,

September.
Priestley, M.J.N. (1997), "Displacement-based seismic assessment of reinforced concrete buildings", *J. Earthq. Eng.*, **1**(1), 157-192.
Priestley, M.J.N. and Kowalsky, M.J. (2000), "Direct displacement-based seismic design of concrete buildings", *Bull. N.Z. Nat. Soc. Earthq. Eng.*, **33**(4), 421-444.
Priestley, M.J.N., Calvi, G.M. and Kowalsky, M.J. (2007), *Displacement-based Seismic Design of Structures*, IUSS Press, Pavia, Italy.
Priestley, M.J.N., Grant, D.N. and Blandon, C.A. (2005), "Direct displacement-based seismic design", *Proceedings of New Zealand Society for Earthquake Engineering Conference*, Wairakei, New Zealand, March.
Șadan, O.B., Lorenza, P. and Calvi, G.M. (2013), "Direct displacement-based seismic assessment procedure for multi-span reinforced concrete bridges with single-column piers", *Earthq. Eng. Struct. Dyn.*, **42**(7), 1031-1051.
Sahu, D., Nishanth, M., Dhir, P., Sarkar, S., Davis, R. and Mangalathu, S. (2019), "Stochastic response of reinforced concrete buildings using high dimensional model representation", *Eng. Struct.*, **179**, 412-422.
SEAOC (1995), Vision 2000: Performance based seismic engineering of buildings, Structural Engineers Association of California, Sacramento, California, U.S.
SeismoSignal (2011), A Computer Program for Signal Processing of Strong Motion Data, Available from URL: http://www.seismosoft.com
Singh, M.P. (2006), "Seismic protection of counterweight-rails in elevators in buildings", *Earthq. Eng. Struct. Dyn.*, **35**(3), 385-394.
Smerzini, C., Galasso, C., Iervolino, I. and Paolucci, R. (2014), "Ground motion record selection based on broadband spectral compatibility", *Earthq. Spectra*, **30**(4), 1427-1448.
Tolis, S.V. and Faccioli, E. (1999), "Displacement design spectra", *J. Earthq. Eng.*, **3**(1), 107-125.
Tubaldi, E. and Dall'Asta, A. (2011), "A design method for seismically isolated bridges with abutment restraint", *Eng. Struct.*, **33**(3), 786-795.
Vamvatsikos, D. and Cornell, C.A. (2002), "Incremental dynamic analysis", *Earthq. Eng. Struct. Dyn.*, **31**(3), 491-514.

CC